Supporting Information

Vranceanu et al. 10.1073/pnas.1101003109

SI Materials and Methods

Animals. Normal adult chinchillas (*Chinchilla lanigera*) were used for tomographic studies. Adult Long-Evans rats (*Rattus norvegicus*), weighing 230–330 g, were used for immunochemistry studies. For the development studies, 14 Long-Evans rat pups were studied. Two pups were killed on each day [from birth (postnatal day 0, P0) to P6], one for immunofluorescent studies and the other for transmission electron microscopy (TEM). Procedures involving animals were approved by the Institutional Animal Care and Use Committee at the University of Illinois at Chicago.

Fixation for Tomographic Studies. Five adult chinchillas were deeply anesthetized with Nembutal (80 mg/kg) and perfused transcardially with 200 mL physiological saline containing heparin (2,000 IU) followed by 8 mL/g body weight of a trialdehyde fixative, as described previously (1). After perfusion, vestibular epithelia were dissected in 0.1 M PB at 4 °C.

Electron Microscope Tomography. We used serial sections of chinchilla utricular macula for conventional TEM and for intermediate-voltage electron microscopy (IVEM). Our TEM methods have been described previously (1).

Semithin sections (0.5 μm) for IVEM were sectioned with a diamond Histoknife (Diatome) and serial sections were collected onto Formvar-coated or Formvar/Luxel-coated, carbon-coated, 1 × 2-mm single slot grids (Ted Pella). All sections were stained with 2% (wt/vol) uranyl acetate (10 min) and Sato lead stain (10 min), and then carbon-coated again. Fiducial cues consisting of 20-nm colloidal gold particles were deposited on one side of each section.

We analyzed a total of 41 tomograms using research facilities at the National Center for Microscopy and Imaging Research. For each reconstruction, a series of images at regular tilt increments was collected as described previously (2). Tilt series were recorded with a Gatan 4 K × 4 K camera at 5,000× magnification. We used a magnification of 5,000× to comfortably include the entire circumference of the apical part of type I hair cell, the proximal part of the hair bundle, and most of the type I hair cell constriction (neck) in the field of interest. The *z*-resolution of the tomographic volumes was 8 nm, compared with the 70-nm thickness of ultrathin sections, which allowed us to visualize objects at a much higher effective *z*-depth resolution (8 nm vs. 70 nm) compared with conventional EM. Some elements were reexamined at high magnification (20,000–25,000×).

Three-Dimensional Reconstruction. The pixel sizes in our reconstructions were 2.8 nm and 1.96 nm. The IMOD software package (3) was used for rough alignment, and in some cases for fine alignment and reconstruction. Warped reconstructions were processed (fine alignment and reconstruction) using the TxBR software package (4). Serial tomograms of hair cells were joined using Etomo (IMOD) and four final volumes were obtained: three type I hair cells, (cell 1 from 6 serial tomograms, cell 2 from 11 serial tomograms, and cell 3 from 5 serial tomograms), and one type II hair cell (cell 4, from 9 serial tomograms). For each final volume (tomogram), segmentation was performed by manual tracing in the planes of highest resolution and by automated isosurface rendering with the program 3dmod (IMOD). Reconstructions were visualized using 3dmod. Cell 5, a striolar type I hair cell, and cell 6, an extrastriolar type II hair cell, were visualized with 3dmod as eight and three serial tomograms, respectively, but not segmented. The program allows stepping through slices of the reconstruction in any orientation (SLICER option) and tracking or modeling features of interest in any of the three dimensions. For quantification, measurements were made using 3dmod ("Object info" feature). Stereocilia and rootlet perimeters were each measured at the same distance above the cell membrane (5.6 nm), and the volumes and surface areas of mitochondria below the cuticular plate within 6 μm of the apical surface of hair cell were also measured. Movies of surface-rendered volumes and slices through the reconstructions were made using Amira software (version 5.2.1, Mercury/TGS).

EM Immunogold Quantification. To test if there were a nonuniform distribution of particles, we examined 14 striated organelles (SO) profiles from 12 hair cells (five type I and seven type II) and divided them into intervals. Starting with each thick filament, an interval was divided into eight equally spaced samples running parallel to the thick filaments, and we determined the interval into which each particle fell. A χ^2 test of homogeneity using "a single classification with equal expectations" ($\chi^2 = 23.1$, $df = 7$, $P < 0.002$) indicated a preference for the intervals immediately adjacent to the thick filament.

Antibodies. Primary antibodies used were: mouse anti α-2 spectrin (Chemicon), goat anti-calretinin (Chemicon). Secondary antibodies for confocal experiments (Chemicon) were: Alexa 488-conjugated donkey anti-goat; Alexa-594-conjugated donkey anti-mouse. Secondary antibody for EM immunogold experiments (Aurion kit, EM Sciences) was: gold-conjugated rabbit anti-mouse. We used calretinin antibody as a marker of hair-cell type (5).

Immunohistochemistry. Three animals were used for immunohistochemical studies and three for Western blots. Fixation, confocal microscopy, and EM immunogold procedures were identical to those described in a recent study (5), which can be consulted for details. Western blots were done to verify that the hair-cell staining found in rat endorgans was α-2 spectrin. For Western blots, animals were anesthetized (Nembutal, 80 mg/kg, i.p.) and decapitated. Vestibular endorgans, cochleae, vestibular ganglion, brain (positive control), and vibrissae (negative control) were harvested from three adult rats within 10 min of killing. Methods were identical to those published previously (5), except that the ECL detection kit was obtained from GE Healthcare Life Sciences. Antibody incubation conditions were mouse anti–α-2 spectrin antibody (diluted 1:2,000) for 4 h at room temperature, washed 3 × 5 min in PBS-Tween, and HRP-conjugated goat anti-mouse IgG (diluted 1:30,000) for 1 h at room temperature. The identities of bands from Western blots were confirmed with mass spectrometry in the University of Illinois at Chicago Proteomics Laboratory. Scaffold software (v.3.1.4.1, Proteome Software) was used to validate mass spectrometry-based peptide and protein identifications.

Mass Spectrometry. Analysis was performed by the University of Illinois at Chicago Research Resources Center's Mass Spectrometry, Metabolomics, and Proteomics Facility. The in-gel tryptic digestion was performed according to the protocol described by Kinter and Sherman (6). Briefly, the gel bands were cut into 1-mm^3 pieces, rinsed, and dehydrated. The protein was reduced with DTT and alkylated with iodoacetamide in the dark, before overnight digestion with trypsin at 37 °C in 50 mM ammonium bicarbonate. Peptides were concentrated and analyzed with a Thermo Orbitrap Velos mass spectrometer using a chip-based HPLC system (Agi-

lent Chip Cube) adapted to run on the Orbitrap Velos (7) using collision-induced dissociation fragmentation.

Database Searching. Tandem mass spectra were extracted by Readw.exe (version 4.0.2, Institute for Systems Biology), converted to the Mascot generic format using MzXML2Search and then submitted to a Mascot search engine (version 2.2.04). Charge state deconvolution and deisotoping were not performed. Mascot was set up to search the SwissProt 57.15 database (selected for *Rattus* taxonomy), assuming the digestion enzyme was trypsin. Mascot was searched with a fragment ion mass tolerance of 0.60 Da and a parent ion tolerance of 10.0 ppm. Oxidation of methionine, acetylation of lysine, and the N terminus and iodoacetamide derivative of cysteine were specified in Mascot as variable modifications.

Criteria for Protein Identification. Scaffold software (v. 3.1.4.1, Proteome Software) was used to validate MS/MS-based peptide and protein identifications. Peptide identifications were accepted if they could be established at greater than 95.0% probability as specified by the Peptide Prophet algorithm (8) and if they contained at least two identified peptides. Protein probabilities were assigned by the Protein Prophet algorithm (9). Proteins that contained similar peptides and could not be differentiated based on MS/MS analysis alone were grouped to satisfy the principles of parsimony.

1. Lysakowski A, Goldberg JM (1997) A regional ultrastructural analysis of the cellular and synaptic architecture in the chinchilla cristae ampullares. *J Comp Neurol* 389:419–443.
2. Perkins GA, et al. (2010) The micro-architecture of mitochondria at active zones: Electron tomography reveals novel anchoring scaffolds and cristae structured for high-rate metabolism. *J Neurosci* 30:1015–1026.
3. Kremer JR, Mastronarde DN, McIntosh JR (1996) Computer visualization of three-dimensional image data using IMOD. *J Struct Biol* 116:71–76.
4. Lawrence A, Bouwer JC, Perkins G, Ellisman MH (2006) Transform-based backprojection for volume reconstruction of large format electron microscope tilt series. *J Struct Biol* 154:144–167.
5. Lysakowski A, et al. (2011) Molecular microdomains in a sensory terminal, the vestibular calyx ending. *J Neurosci* 31:10101–10114.
6. Kinter M, Sherman NE (2000) *Protein Sequencing and Identification Using Tandem Mass Spectrometry* (Wiley-Interscience, New York), pp 152–160.
7. Schilling AB, Crot C, Helseth DL, Xu H, Davis RG (2010) Conversion of an Agilent Chip Cube system for the analysis of proteomics samples using a LTQ-FT Ultra mass spectrometer. *58th ASMS Conference on Mass Spectrometry, Salt Lake City, UT May 24–27, 2010*, Poster # MP612.
8. Keller A, Nesvizhskii AI, Kolker E, Aebersold R (2002) Empirical statistical model to estimate the accuracy of peptide identifications made by MS/MS and database search. *Anal Chem* 74:5383–5392.
9. Nesvizhskii AI, Keller A, Kolker E, Aebersold R (2003) A statistical model for identifying proteins by tandem mass spectrometry. *Anal Chem* 75:4646–4658.

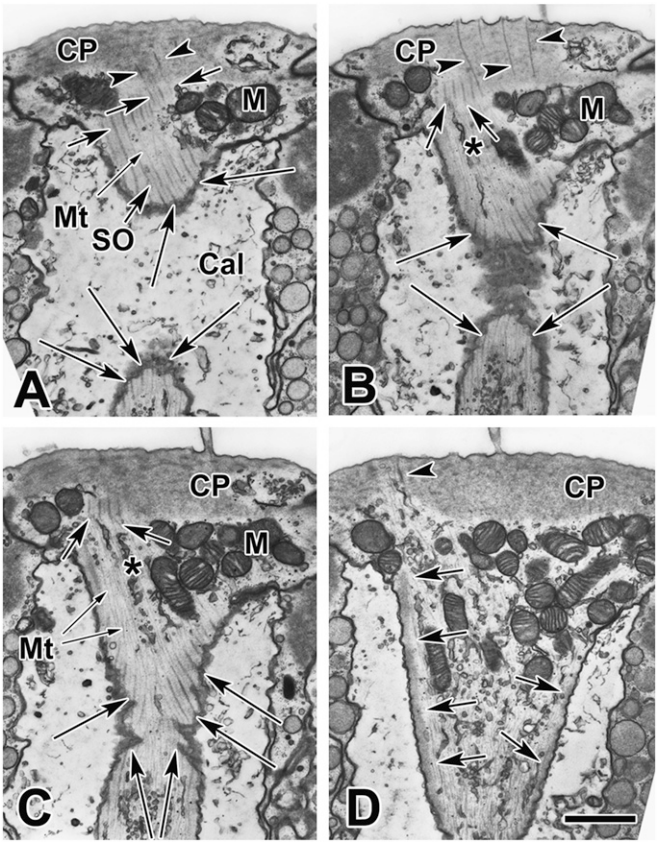

Fig. S1. Serial section TEM of SOs. Ultrathin sections from a serial section study of type I vestibular hair cells in chinchilla crista. (*A* and *B*) Actin stereociliar rootlets (SR) in a striolar type I hair cell are directly continuous with stereocilia (arrowheads) and enter the SO (SO, short arrows). In the lower part of the neck, long arrows show insertions of the thick SO filaments into the cell membrane. Some microtubules (Mt, long, thin arrows) in *A* and *C* connect SRs to the SO below the central portion of the cuticular plate. Vesicular structures (asterisks in *B* and *C*) line up in parallel with microtubules (Mt) and the SO. (*D*) Section through the median plane of a type I hair cell, showing gray bands (short arrows) that lie between the thick filaments of the SO forming a narrow band along the cell membrane. Our EM immunogold results indicate this gray band is α-2 spectrin. (Scale bar in *D*, 1 μm; applies to all panels.) CP, cuticular plate; M, mitochondria.

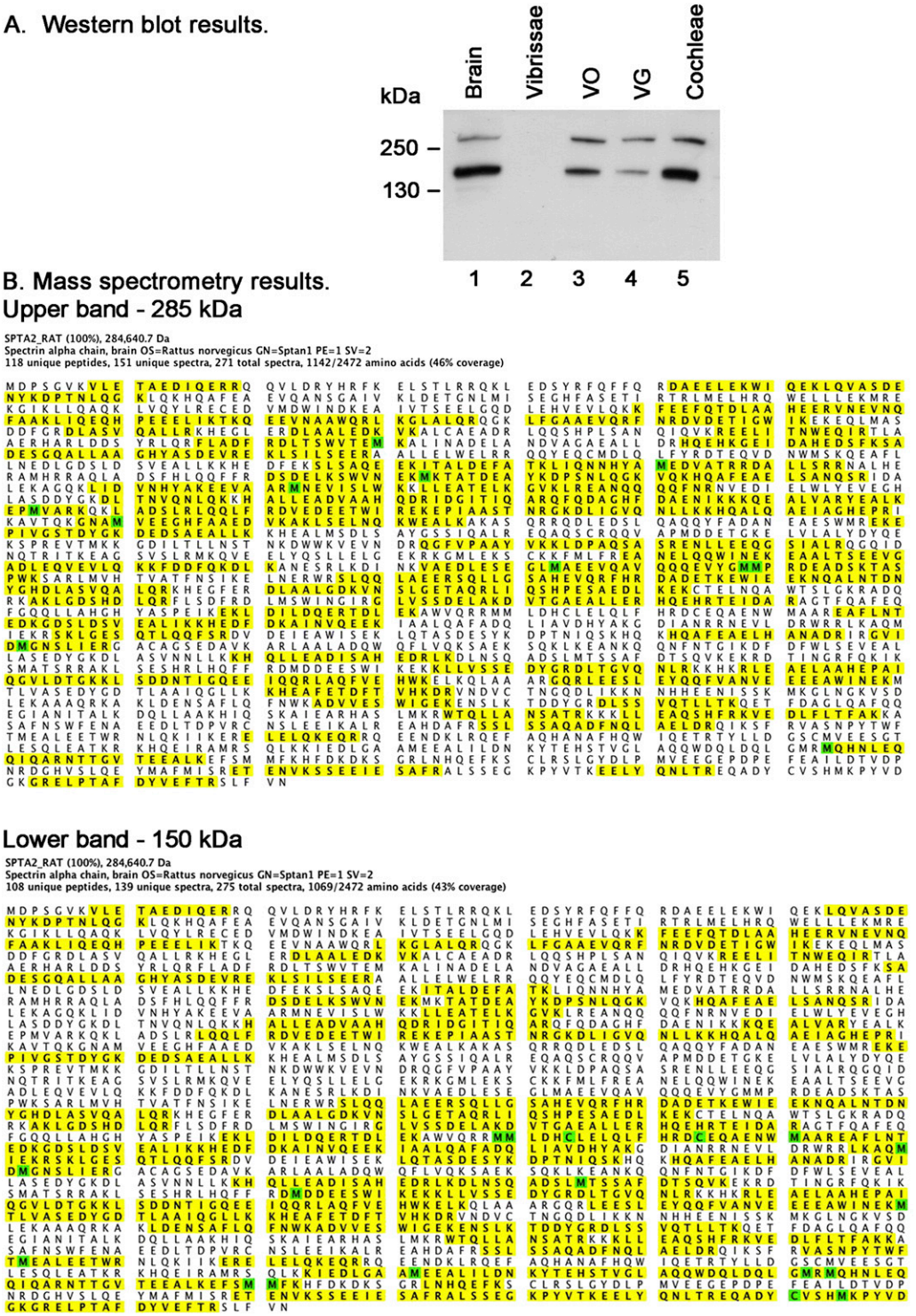

Fig. S2. Antibody validation. (*A*) Immunoblot of rat brain (positive control for α-2 spectrin), vibrissae (negative control), vestibular end organs (VO), vestibular ganglia (VG), and rat cochleae labeled with an anti–α-2 spectrin antibody. The blot shows two spectrin bands. The upper band corresponds to the full-length α-2 spectrin protein (285 kDa), the lower band to a well-characterized proteolytic fragment at ∼150 kDa (1). (*B*) Mass spectrometry results. (*Upper*) Results of our mass spectrometry runs on the upper (285 kDa) band in our immunoprecipitation gels. With 46% coverage and 118 unique peptides, there is 95–100% confidence that the band is α-2 spectrin. (*Lower*) Results of mass spec runs on the lower, 150-kDa band in our gels. Again, with 43% coverage and 108 unique peptides, there is a similar level of confidence that this band is also α-2 spectrin.

1. Harris AS, Croall DE, Morrow JS (1988) The calmodulin-binding site in alpha-fodrin is near the calcium-dependent protease-I cleavage site. *J Biol Chem* 263:15754–15761.

Table S1. Subcuticular mitochondrial dimensions

	Type I hair cells				Neighboring type II hair cells			
Samples	*n*	SA (10^6 nm^2)	Vol (10^8 nm^3)	SA/Vol ratio	*N*	SA (10^6 nm^2)	Vol (10^8 nm^3)	SA/Vol ratio
Cell 1 juxtastriolar	14	1.74 ± 0.79	1.46 ± 0.61	0.012	12	0.90 ± 0.56	0.45 ± 0.29	0.020
Cell 2 extrastriolar	29	1.58 ± 0.73	1.61 ± 1.05	0.010	15	0.75 ± 0.36	0.38 ± 0.19	0.020
Cell 3 extrastriolar	13	1.61 ± 0.81	1.39 ± 0.92	0.012	10	0.95 ± 0.56	0.40 ± 0.21	0.024
Average	56	1.64 ± 0.09	1.49 ± 0.11	0.011	37	0.87 ± 0.10	0.41 ± 0.04	0.021

Samples, region and cell number from which samples were taken; *n,* number of mitochondria measured for each type of cell; Values, mean ± SD. Only complete mitochondria from the subcuticular region (~6 μm below the apical cell membrane) in type I and neighboring type II hair cells were reconstructed. As mitochondrial function is related to overall size (in particular to surface area), mean volumes (Vol) and surface areas (SA) were measured for each organelle, and surface to volume ratios (SA/Vol) were calculated. Student *t* test was used to compute significance levels for type I vs. type II mitochondrial surface areas ($P < 0.0001$) and volumes ($P < 0.0001$).

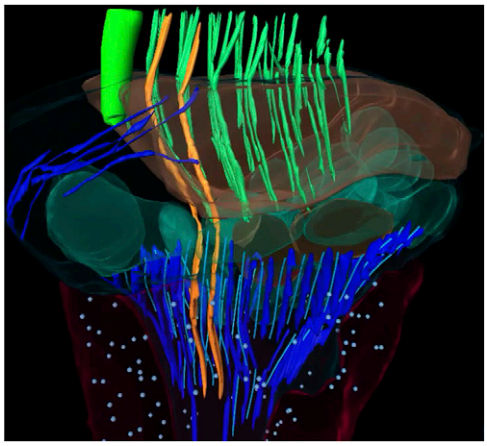

Movie S1. Movie showing digital sections through the tomogram (six serial semithin sections at 0.5 μm per section, a total of 3 μm joined volume) and presentation of modeled apical structures from cell 1 (a juxtastriolar type I hair cell): hair-cell membrane, cuticular plate, subcuticular mitochondria, kinocilium, SRs, SO—thick and thin filaments—and connections between SRs and SO. Extracellular structures: calyx terminal, containing dense core vesicles. All labels have been colored to match the color-coding of each modeled structure.

Movie S1

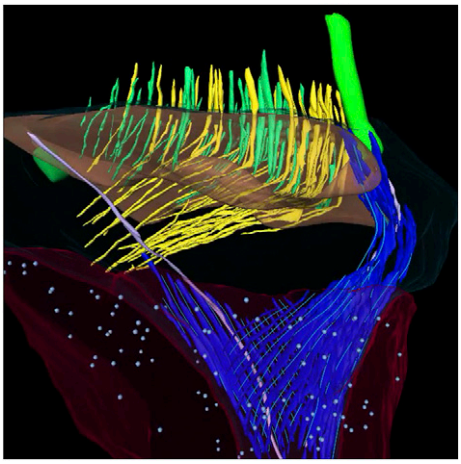

Movie S2. Movie showing digital sections through the tomogram (11 serial semithin sections at 0.5 μm per section, a total of 5.5 μm of joined volume) and presentation of apical structures modeled from cell 2 (an extrastriolar type I hair cell): hair cell membrane, cuticular plate, subcuticular mitochondria, kinocilium, SRs, centriole and kinociliar rootlets, SO—thick and thin filaments—and SRIA (SR inserting areas). Extracellular structures: calyx terminal, containing dense core vesicles. Labels have been colored to match the color-coding of each modeled structure.

Movie S2